MODELING COASTAL WATER CLARITY USING LANDSAT-8 AND SENTINEL-2

Sarah Lang*, **Dr. Max C.N. Castorani***, **Dr. Scott C. Doney***

* Department of Environmental Sciences, University of Virginia

ABSTRACT

Understanding and attributing changes to water quality is essential to the study and management of coastal ecosystems and functions they sustain. However, measuring water clarity—a key aspect of water quality—is challenging because it varies greatly over space and time due to natural and anthropogenic processes. Coupling long-term *in situ* observations with estimates from satellite algorithms could provide a more complete understanding of coastal water clarity changes and its drivers. Here, we created a remote sensing product by coupling Landsat-8 and Sentinel-2 reflectance data with water clarity measurements at 7 sites over 8 years in a shallow turbid coastal lagoon system in Virginia, USA. Our satellite-based model explained 29% of the variation in *in situ* water clarity, and an out-of-sample validation showed that the model accurately represented interannual variability. Our product increases the spatiotemporal scope of *in situ* water clarity data and improves estimates from bio-optical algorithms that overpredicted water clarity. Our results demonstrate the ability of high-resolution satellite imagery to improve estimates of coastal water clarity and highlight the need to further improve and calibrate ocean color algorithms for complex water bodies.

1. INTRODUCTION

Measuring and predicting coastal water quality variability is valuable for the understanding and management of marine and estuarine ecosystems (Álvarez-Romero et al., 2014). For example, understanding changes in water clarity can aid the restoration and preservation of benthic habitats and submerged aquatic vegetation, which are often limited by light (Carr et al., 2010). However, studying coastal water quality is challenging because it is highly variable across a range of scale in space and time due to natural and anthropogenic processes (Bierman et al., 2009). Long-term measurements offer one important tool in describing and forecasting water quality, but for logistical reasons are limited in spatiotemporal dimensions

Water clarity—a key component of water quality—has historically been measured by Secchi disks, black and white painted disks that are lowered into the water until they are no longer visible from the surface (Preisendorfer, 1986). Secchi disks serve as a reliable and low-cost way to determining the amount of optically active constituents in the water column (ie. phytoplankton, detritus, color dissolved organic matter, inorganic particles). These measurements have helped document historical water clarity changes, like in the coastal seaside lagoons of Virginia's Eastern Shore (McGlathery and Christian, 2020). However, *in situ* water clarity measurements cannot fully capture variability alone. Much time and effort are needed to collect the data and there are large spatiotemporal gaps due to sampling limitations. Coupling remotely-sensed satellite measurements with *in situ* measurements could provide a more complete understanding of water quality changes and drivers in coastal ecosystems, as well as a way to separate directional changes from natural variability.

Biogeochemical parameters like Secchi depths (Lee et al., 2016) can be estimated by satellites measuring visible light emitted by the water, or ocean color (Werdell and McClain, 2019). Ocean color data can be extremely helpful in studying coastal waters on a synoptic scale; however, these environments pose unique challenges to ocean color remote sensing. High concentrations of particulate organic matter, proximity to land, backscattering from shallow waters, bubbles from breaking waves, etc. affect bio-optical measurements (Loisel et al., 2013). Validation with *in situ* measurements is crucial before implementing ocean color algorithms in any water body, but these challenges make it especially important to test algorithms in a wide range of coastal oceans.

Another unique challenge associated with coastal ocean remote sensing is the need for high resolution satellite data that traditional ocean color sensors have too coarse spatial resolutions (~1 km or more) to capture. The Landsat-8's Operational Land Imager (OLI) and the Sentinel-2's MultiSpectral Instrument (MSI) have moderate-to-high spatial resolutions (Landsat-8: Coastal aerosol (~443 nm), Blue (~482 nm), Green (~561 nm), and Red (~655 nm): 30 m; Sentinel-2: Coastal aerosol (~443 nm): 60 m; Blue (~492 nm), Green (~560 nm), and Red (~665 nm): 10 m) that allow for observations in coastal environments. Cross-calibration of the two sensors during the development of the satellites led to compatible data products (ESA, 2013). The benefit of combining these observations has been demonstrated in recent literature; for example, NASA's Harmonized Landsat Sentinel-2 project shows that using the two satellites in unison increases the temporal resolution and accuracy of the data (https://hls.gsfc.nasa.gov/).

The Lee et al. Landsat-8 semi-analytical Secchi depth (Z_{SD}) model has been applied to various water bodies globally and recalibrated to improve its accuracy in various water types (Lee et al., 2016; Chen et al., 2019; Liu et al., 2019; Luis et al., 2019). Luis et al. demonstrated that the model can be applied to a range of coastal water bodies; however, algorithm evaluation using *in situ* data is still needed to improve the algorithm (Luis et al., 2019). This algorithm has yet to be applied to Virginia's Eastern Shore, where extensive *in situ* water quality measurements by the Virginia Coast Reserve Long Term Ecological Research project (VCR LTER) provide a unique opportunity for algorithm evaluation, as well as an opportunity to extend the spatiotemporal scope of this data (McGlathery and Christian, 2020). Additionally, we seek to determine if the algorithm is compatible with the Sentinel-2, which would greatly increase the temporal resolution of satellite data.

2. METHODS

2.1 Overview

We compared satellite-derived Secchi depths from the Lee et al. 2016 Z_{SD} algorithm with *in situ* measurements, using a time window of ± 0-8 days between satellite overpass and *in situ* sampling to yield a sufficient number of *in situ*-satellite matchups. There was no evidence that the size of the window affected the results in a statistically significant way. The satellite algorithm overestimated Secchi depths ($Z_{SD,sat}$) relative to their corresponding *in situ* values ($Z_{SD,insitu}$), so we created a new model with multiple regression to predict more accurate Secchi depths ($Z_{SD,model}$). Our model was evaluated using root mean square error (RMSE), mean absolute percent difference (MAPD), and time series modeling as an out of sample validation. We used general additive models to model time series in order to determine if $Z_{SD,model}$ could capture the interannual variability and seasonal trends as shown by $Z_{SD,insitu}$. Furthermore, we investigated differences in Landsat-8/Sentinel-2 retrievals, as well as differences between NASA SeaDAS (https://seadas.gsfc.nasa.gov/) and an alternative atmospheric correction method for coastal waters, ACOLITE (https://odnature.naturalsciences.be/remsem/software-and-data/acolite).

2.2 Study System and *In Situ* Data Collection

We focused our investigation on a coastal lagoon system studied by the Virginia Coast Reserve Long Term Ecological Research Project (VCR LTER) located in Virginia, USA, near the southern tip of the Delmarva Peninsula (Fig. 1). Due to low nitrogen inputs and frequent exchange with the Atlantic Ocean via inlets between barrier islands (Fig. 1), water quality is high relative to coastal bays in the United States and worldwide (McGlathery et al., 2007). Since 1992, VCR LTER researchers have collected Secchi depths and other water-quality parameters at 17 sites that include tidal flats (0-2 m depth), deep flats (2-4 m depth), and deeper oceanic inlets and channels (>4 m depth) (Safak et al., 2015). Sampling was carried out monthly from 1998 to 2008 and quarterly from 2008 to 2020 (McGlathery and Christian, 2020).

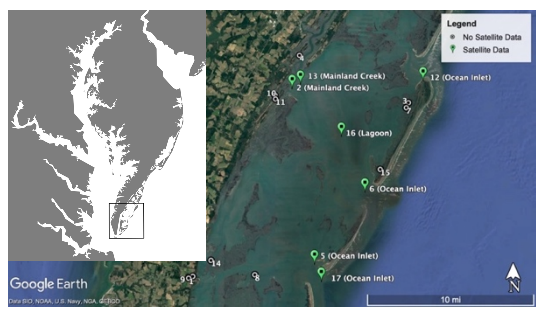

Figure 1: Map of the 17 tested sites with in situ Secchi depth data. Green markers indicate that remote sensing reflectances could be captured at the site.

2.3 Satellite Data

To retrieve remote sensing reflectances (R_{rs}, sr^{-1}) to calculate satellite-derived Secchi depths, we collected images from Landsat-8 and Sentinel-2 satellites. We used USGS Earth Explorer (https://earthexplorer.usgs.gov/, Accessed June 2019-November 2020) to collect Level-1 Landsat-8 images (https://doi.org/10.5066/F71835S6) and The Copernicus Open Access Hub (ESA, https://scihub.copernicus.eu/, Accessed June 2020-November 2020) to collect Level-1 Sentinel-2 images. The Sentinel-2A and 2B are identical polar orbiting satellites phased at 180˚ to each other, resulting in a high revisit time of 2-3 days at mid-latitudes. Landsat-8 has a 16-day revisit time. We generated remote sensing reflectances by processing Level-1 images and implementing atmospheric corrections and ocean color algorithms with the l2gen program in NASA SeaDAS. The NASA standard NIR-band algorithm was used for atmospheric correction for bands 5 and 7 (865 nm and 2201 nm) applicable for coastal waters (Wei et al., 2018). The standard Level-2 quality flags were masked, including ATM (atmospheric correction failure), LAND (land pixel), CLDICE (probable cloud or ice contamination), and HILT (very high or saturated radiance). The bidirectional reflectance distribution function (BRDF) of Morel et al. was implemented (2002).

We used the Quasi-Analytical Algorithm (v6) to derive inherent optical properties (IOPs), total absorption (*a*) and backscattering (*bb*) coefficients from the multi-spectral R_{rs} spectrum (Lee et al. 2002). The Landsat-8's spectrum includes center wavelengths at ~443, 482, 561, and 655 nm, and the Sentinel-2's spectrum includes center wavelengths at ~443, 492, 560, and 665 nm. We then derived diffuse attenuation coefficients (K_d, m^{-1}) from the IOPs. $K_d(530)$ was determined empirically by the methods of Lee et al. in order to fill the large spectral gap between 482 and 561 nm (Lee et al. 2015). K_d at the transparent window, the minimum K_d value, and the R_{rs} value at the corresponding wavelength were used to find the satellite Secchi depth ($Z_{SD,sat}$, m) (Lee et al. 2005, 2015, 2016).

$$Z_{SD,sat} = \frac{1}{2.5Min(K_d^{tr})} \ln\left(\frac{0.14 - R_{rs}^{tr}}{0.013}\right) \qquad (1)$$

Valid (not masked by flags) remote sensing reflectances (R_{rs}) from SeaDAS were recovered at 7 of 17 *in situ* sampling sites: 4 ocean inlet sites, 1 lagoon site, and 2 mainland tidal creek sites (Fig. 1). Reflectances were masked out by our choice of flags at other sites, possibly due to atmospheric correction failure, proximity to land, clouds, etc.. At suitable sites, a total of 12 Landsat-8 and 8 Sentinel-2 images were captured within ± 0-8 days of *in situ* sampling, resulting in 97 matchups between satellite observations and *in situ* measurements: 61 observations derived from Landsat and 36 observations derived from Sentinel. The number of observations vary by site and date due to varying cloud cover. If Landsat-8 and Sentinel-2 both captured an image in the ± 0-8 day temporal window centered on *in situ* sampling, the satellite with the overpass closest in time to *in situ* sampling was chosen.

2.4 Satellite Reference Processing and Algorithm Evaluation

Satellite observations were compared to their corresponding *in situ* estimates. The Lee et al. 2016 Z_{SD} algorithm overpredicted Secchi depth values relative to their corresponding *in situ* values by an average factor of ~2. We tested the correlation between $Z_{SD,insitu}$ and $Z_{SD,sat}$ using the "stats" package in R Studio 1.2335 and found a significant correlation ($r = 0.52$, $p < 0.001$) (R Core Team, 2019). Therefore, a statistical model could be useful in reducing systematic biases produced by the Lee et al. Z_{SD} algorithm.

In order to build the predictive model, fixed effects models were explored with the duration between satellite observations and *in situ* sampling, satellite type (Landsat-8 or Sentinel-2), and $Z_{SD,sat}$ (from the Lee et al. algorithm) to predict $Z_{SD,insitu}$. We used the "car" package in R 4.0.3 (R Code Team 2020) to identify the most parsimonious model via backwards model selection based on Type III Sum of Squares (Fox and Weisberg, 2019).

We analyzed models using the "stats" package (R Code Team 2020). We assessed the significance of model terms using *F* tests. We checked for homogeneity of variance by plotting normalized model residuals against model predictions and individual predictors. We ensured normality of residuals using histograms and quantile-quantile plots. We removed one satellite measurement outlier, however model selection and parameters were robust to this decision. We tested for temporal autocorrelation using autocorrelation function analysis; no significant autocorrelation was detected.

2.5 Model Evaluation and Validation

We evaluated how well the remote sensing model could predict Secchi depths by comparing $Z_{SD,model}$ to $Z_{SD,insitu}$ using the root mean square error (RMSE) and the mean absolute percent difference

(MAPD) in the "Metrics" package (Hamner and Frasco, 2018).

$$RMSE = \sqrt{\frac{1}{n}\sum_{i=1}^{n}(x_{model,i} - x_{in\ situ,i})^2} \quad (2)$$

$$MAPD = \frac{1}{n}\sum_{i=1}^{n}\left|\frac{x_{model,i} - x_{in\ situ,i}}{x_{in\ situ,i}}\right| \times\ 100\% \quad (3)$$

We also investigated how well the model-derived observations captured the interannual variability and the seasonal trends in water clarity shown by *in situ* observations. To estimate these trends, we fit generalized additive models (GAMs) with the "mgcv" package in R to two time series: one of modeled Secchi depths ($Z_{SD,model}$) and one of *in situ* Secchi depths ($Z_{SD,insitu}$) (Wood 2017). Both the satellite-model and *in situ* time series were irregularly spaced and had different distributions across time, but GAMs can handle irregularly spaced time series (Simpson 2018).

We used a low-rank thin plate regression spline to model the interannual variation as a function of date (f_1), a cyclic cubic regression spline to model the seasonal Secchi depth as a function of year day (f_2), and a tensor product smooth to account for their interaction (f_3) (Eq. 4). We selected the appropriate number of basis functions by checking the k-indices and p-values with the gam_check() command. Only *in situ* data from 2013-2020 was used to compare trends from the same time period as the satellite data. Additionally, only Landsat-8 measurements were used in this analysis due to the availability of processed Level-2 data.

$$Z_{SD} = \beta_0 + f_1(\text{date}) + f_2(\text{year day}) + f_3(\text{date, year day}) \quad (4)$$

2.6 Satellite Data Assessment

We compared uncorrected Landsat-8 and Sentinel-2 Secchi depths from the Lee et al. 2016 algorithm ($Z_{SD,sat}$) (Eq. 1) and remote sensing reflectances (R_{rs}) from the same day at the same location. We used 6 dates between 2019-2020 and 157 random coordinates sampled using QGIS.

We plotted Landsat-8 $Z_{SD,sat}$ against Sentinel-2 $Z_{SD,sat}$ and compared them with a second order polynomial fit, the most parsimonious model determined by a forward model selection procedure. We also plotted Landsat-8 and Sentinel-2 R_{rs} for bands 1 (443 nm), 2 (Landsat-8: 482 nm, Sentinel-2: 492 nm), 3 (Landsat-8: 561 nm, Sentinel-2: 560 nm), and 4 (665 nm).

REMSEM (Royal Belgian Institute of Natural Sciences) ACOLITE is an alternative to NASA SeaDAS for processing Landsat and Sentinel coastal water imagery. The two processors differ in their atmospheric correction methods, so we sought to determine if using ACOLITE for atmospheric correction would improve the Lee et al. $Z_{SD,sat}$ estimates. Calculations of R_{rs} and $Z_{SD,sat}$ were attempted for all 17 *in situ* sites across 4 Landsat-8 images (9/3/2018, 5/1/2019, 7/20/2019, 07/22/2020). All 17 sites were used to determine if ACOLITE could extract data from sites that SeaDAS consistently masked. Additionally, the anomalously high $Z_{SD,sat}$ that we removed from our model came from the 7/20/2019 image, and we sought to determine if ACOLITE yielded an anomalously high $Z_{SD,sat}$ as well.

3. RESULTS

3.1 Algorithm Evaluation and Model Statistics

The Sentinel-2 and Landsat-8 both predicted *in situ* Secchi depths ($p < 0.001$), although Sentinel-2 predicted *in situ* Secchi depths more accurately than Landsat-8 ($R^2 = 45\%$ vs. $R^2 = 10\%$). The best model included $Z_{SD,sat}$ (m^{-1}), satellite type, and their interaction:

$$\begin{gathered} Z_{SD,model} = 0.15489\ Z_{SD,sat} + 0.47876 + \Delta \\ \Delta_{Landsat} = 0 \\ \Delta_{Sentinel} = 0.18640\ Z_{SD,sat} - 0.26679 \end{gathered} \quad (5)$$

where $Z_{sd,model}$ (m^{-1}) is the model-modified Secchi depth and $\Delta_{Sentinel}$ denotes the correction for the Sentinel-2 satellite.

The satellites differed in their slopes, with Sentinel-2 having a higher slope than Landsat-8 ($b = 0.34$ vs. $b = 0.15$) and yielding predictions closer to the 1:1. In both cases, the slopes were less than 1 because estimated Secchi depth was higher than observed Secchi depth. The multiple regression model could explain 29% of the variance in $Z_{SD,insitu}$ (Table 1) and could predict $Z_{SD,insitu}$ with a root mean square error of 0.20 m and a mean absolute percent difference of 25% (Figure 2). This is an improvement over the unadjusted Lee et al. model (RMSE = 0.92 m, MAPD = 125%).

Table 1: Regression results using $Z_{SD,insitu}$ as the criterion

Predictor	*b*	*b* 95% CI [LL, UL]	sr^2	sr^2 95% CI [LL, UL]
Intercept	0.48**	[0.30, 0.66]		
sat	0.15*	[0.03, 0.27]	.05	[-.02, .12]
typeS2	-0.27	[-0.56, 0.03]	.02	[-.03, .08]
sat:typeS2	0.19*	[0.01, 0.36]	.03	[-.03, .09]

Fit: R^2 = 308**, : R_{adj}^2 = 0.285**, 95% CI[.14,.42]

Note. A significant b-weight indicates the semi-partial correlation is also significant. b represents unstandardized regression weights. sr^2 represents the semi-partial correlation squared. LL and UL indicate the lower and upper limits of a confidence interval, respectively.

Table 2: Fixed-Effects ANOVA results using $Z_{SD,insitu}$ as the criterion

Predictor	Sum of Squares	*df*	Mean Square	*F*	*p*
(Intercept)	1.19	1	1.19	27.59	.000
sat	0.28	1	0.28	6.57	.012
type	0.14	1	0.14	3.27	.074
sat x type	0.19	1	0.19	4.51	.036
Error	3.97	92	0.04		

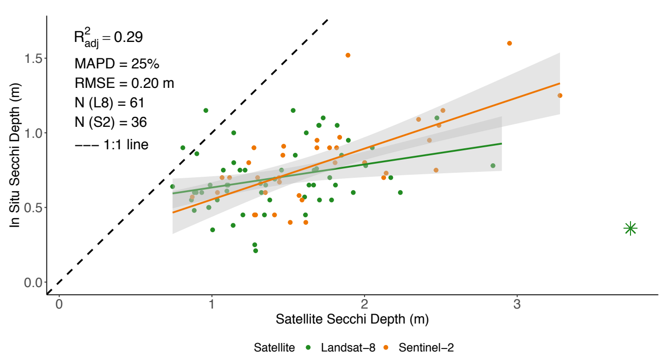

Figure 2: $Z_{SD,sat}$ from Landsat-8 (green) and Sentinel-2 (orange) plotted against $Z_{SD,insitu}$. 95% confidence intervals are plotted in gray. Green asterisk denotes the removed outlier from the Landsat-8.

Deviation from the fit line was similar among sites, with the exception of one relatively shallow site (average depth ~ 5.6 m) located near a mainland creek ("Site 2" in Fig. 4). This explains the large error observed at mainland creek sites (Figure 3B). The model had comparable performances across the rest of the sites, which varied in average depth. For example, a site with a comparable average depth ("Site 5" in Fig. 4, ~ 8.8 m) to the shallow mainland creek site had a similar model performance to the deepest sites ("Site 6," "Site 12", and "Site 17" in Fig. 4, ~ 40-50 m). Sites with intermediate average depths ("Site 13" and "Site 16" in Fig. 4, ~ 20-25 m) had similar performances as well, although within-site replication is low for one of these sites ("Site 13" in Fig. 4).

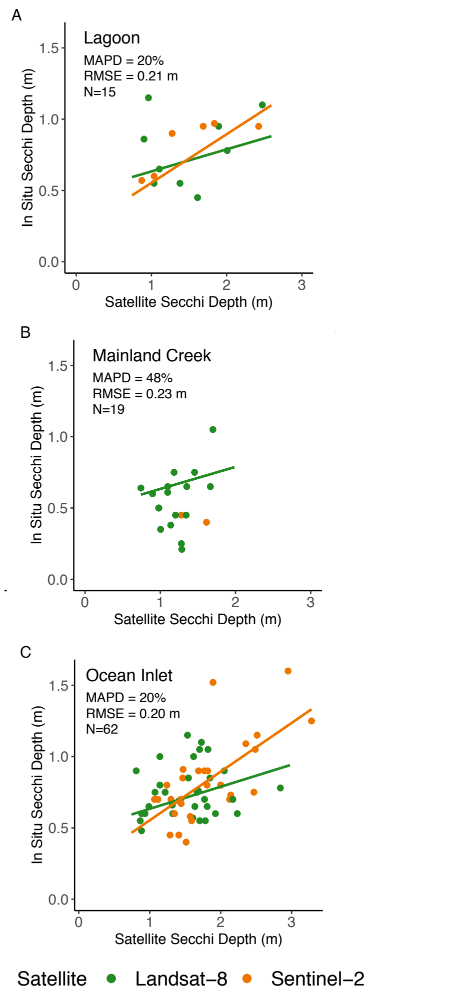

Figure 3: $Z_{SD,sat}$ from Landsat-8 (green) and Sentinel-2 (orange) plotted against $Z_{SD,insitu}$ for each site type. Site 6 is a lagoon, sites 2 and 13 are mainland creeks, and sites 5,6,12, and 17 are ocean inlets. Prediction lines are plotted. MAPD and RMSE are reported for each region.

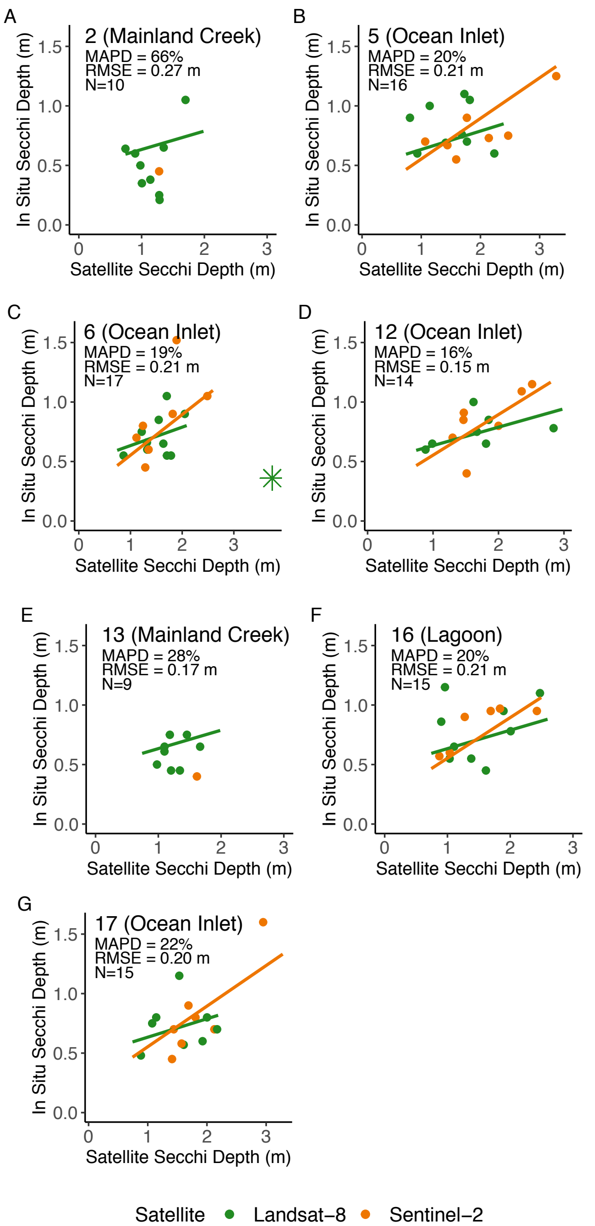

Figure 4: $Z_{SD,sat}$ from Landsat-8 (green) and Sentinel-2 (orange) plotted against $Z_{SD,insitu}$ for each site. Landsat-8 (green) and Sentinel-2 (orange) prediction lines are plotted. MAPD and RMSE are reported for each site.

3.2 Out of Sample Validation

The model captures the interannual variability as shown by *in situ* values. Both dip around 2015 and peak around 2018 (Figure 5 A-B). However, the *in situ* data change more year to year (F = 2.736, p = 0.024) than the modeled data (F = 2.044, p = 0.071). *In situ* and model-derived Secchi depths varied throughout the year ($p < 0.001$), but the correspondence between the two were less clear (Figure 5 C-D). It appears that both dip in June, peak in August, and dip in October, but that their patterns diverge in the winter months.

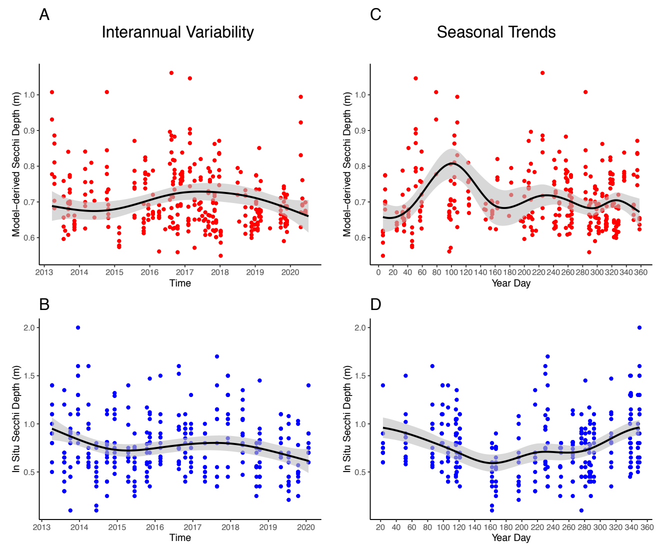

Figure 5: Thin plate regression splines model the relative variation in Secchi depths from year to year (A,B). *Cyclic cubic splines model the seasonal variation in Secchi depth (C,D). $Z_{SD,model}$ values* (A,C) *are shown in red and $Z_{SD,insitu}$ values (B,D) are shown in blue. The splines are shown in black and plotted with their 95% confidence intervals in gray. Note that the $Z_{SD,model}$ time series have different axes than the $Z_{SD,insitu}$ time series because $Z_{SD,insitu}$ have a larger spread than $Z_{SD,model}$.*

3.3 Satellite Data Assessment

The Sentinel-2 yielded higher Secchi depth values than Landsat-8 (Figure 6A), but they had a strong relationship with one another (R^2_{adj} = 0.90, F(2, 238)=1091, p<0.001). Higher Sentinel-2 Secchi depths correspond to lower R_{rs} values for all four visible bands: band 1 (Coastal Aerosol, ~443 nm), band 2 (Blue, ~482 nm), band 3 (Green, ~561 nm), and band 4 (Red, ~665 nm) (Figures 6B-6D).

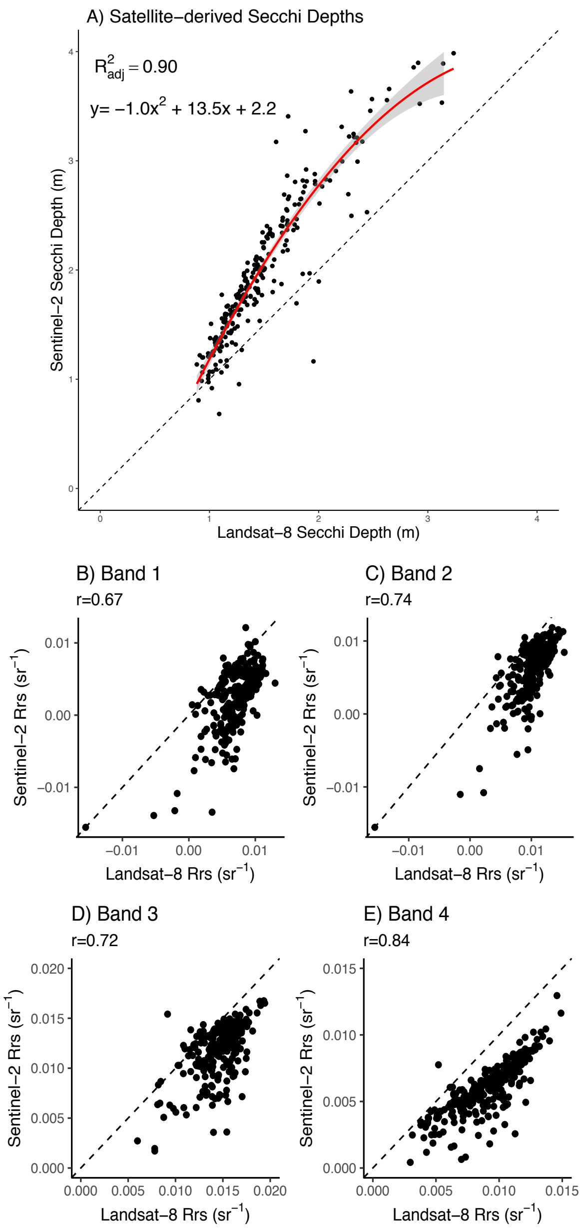

Figure 6: Panel A shows Sentinel-2 $Z_{SD,sat}$ (y-axis) plotted against Landsat-8 $Z_{SD,sat}$ (x-axis). Landsat-8 $Z_{SD,sat}$ explains 90% of the variation in Sentinel-2 $Z_{SD,sat}$. Sentinel-2 yields higher $Z_{SD,sat}$ than Landsat-8 (A). Sentinel-2 yields lower R_{rs} values for all four bands (Band 1: Coastal Aerosol, Band 2: Blue, Band 3: Green, Band 4: Red). Pearson product moment correlation coefficients are denoted by r (B-E).

Like NASA SeaDAS, REMSEM ACOLITE can predict *in situ* Secchi depths (p = 0.021). NASA SeaDAS yields higher Secchi depth values (x̄ = 1.64 m, s = 0.43 m) than REMSEM ACOLITE (x̄ = 0.990 m, s = 0.16 m), but SeaDAS $Z_{SD,sat}$ explain more variation in *in situ* Secchi depths than ACOLITE $Z_{SD,sat}$ (R^2 = 24% vs. R^2 = 15%). Lower $Z_{SD,sat}$ values from ACOLITE correspond to higher R_{rs} values (Figures 7 and 8).

ACOLITE also yielded an anomalously high $Z_{SD,sat}$ ($Z_{SD,sat}$=1.77 m) where NASA SeaDAS yielded an outlier ($Z_{SD,sat}$=3.74 m, $Z_{SD,insitu}$=0.36 m) (Figure 7). The anomalously high $Z_{SD,sat}$ corresponds to an anomalously low R_{rs}(665) (Figure 8).

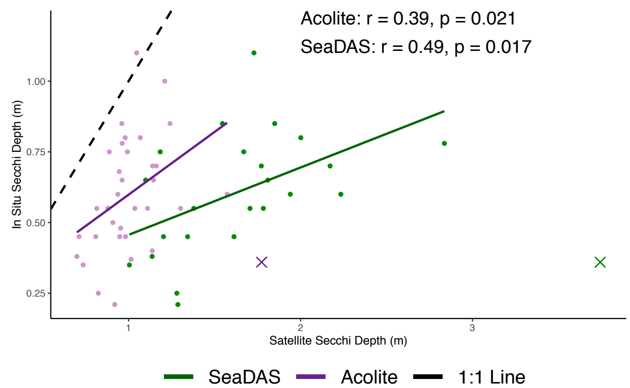

Figure 7: $Z_{SD,sat}$ calculated with NASA SeaDAS R_{rs} (green) plotted against $Z_{SD,sat}$ from REMSEM ACOLITE R_{rs} (purple). ACOLITE yields lower $Z_{SD,sat}$. Anomalously high $Z_{SD,sat}$ from ACOLITE and SeaDAS denoted by the symbol ×. 1:1 line is plotted with a dotted line.

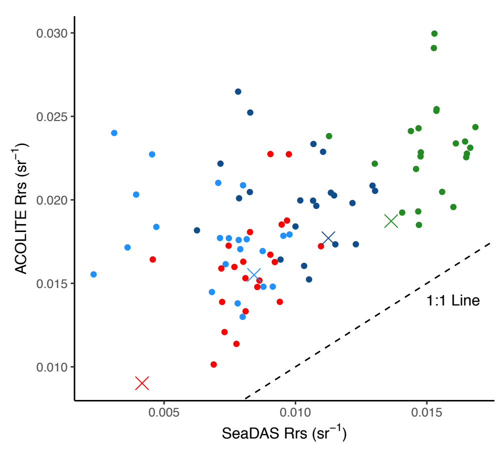

Figure 8: SeaDAS R_{rs} plotted against ACOLITE R_{rs}. ACOLITE yields higher R_{rs}. Anomalously high R_{rs} from ACOLITE and SeaDAS denoted by the symbol ×. 1:1 line is plotted with a dotted line.

4. DISCUSSION

We created a remote sensing product that increases the spatiotemporal scope of the *in situ* water clarity data and improves estimates from bio-optical algorithms that overestimated water clarity. Our modeling methods can be used to yield more accurate Secchi depth values in other coastal oceans where inaccurate $Z_{SD,sat}$ is observed. Furthermore, identifying and correcting the ocean color algorithm causing inaccuracies in Secchi depth estimates could lead to the better understanding of the optical properties of coastal waters, and therefore the improvement of coastal ocean satellite remote sensing. This investigation could include the use of alternative R_{rs} to IOP algorithms or alternative atmospheric correction methods. Another useful future direction for this research would be to use our model to study spatial variation in water clarity, as well as temporal variation over seasonal to interannual time scales.

4.1 Model Assessment

The model improved Secchi depth estimates relative to the unadjusted Lee et al. Z_{SD} model for both the Landsat-8 and Sentinel-2 satellites. The similar model performance among sites indicates that the model can be generalized to any location within the VCR. As for the data used to build the model, SeaDAS was the better atmospheric correction method to obtain measurements for modeling because it could explain more variation in *in situ* Secchi depths than ACOLITE. Additionally, the strong relationship between Landsat-8 and Sentinel-2 measurements demonstrates the compatibility of their data products.

4.2 Using Sentinel-2 Data in Conjunction with Landsat-8 Data

We found that the Sentinel-2 yields larger Secchi depth values and lower R_{rs} values than the Landsat-8 consistently, suggesting that differences in values are most likely due to inherent satellite product differences rather than environmental factors (eg. tidal differences occurring in the temporal window between overpasses). Sentinel-2 has been found to yield lower reflectance values than Landsat-8 because Sentinel-2 products are not vicariously calibrated with *in situ* optical measurements like the Landsat-8's products (Pahlevan et al. 2017). However, environmental factors cannot be ruled out until they are further investigated. Additionally, Sentinel-2 $Z_{SD,sat}$ had a higher correlation with $Z_{SD,insitu,}$ than Landsat-8 $Z_{SD,\mathrm{sat}}$, despite the formula being optimized for Landsat-8.

Another consideration regarding the merger of Landsat/Sentinel data is the parametrization of the algorithm for M30 products from NASA's Harmonized Landsat Sentinel project (Masek, 2018). M30 products are seamless surface reflectances with 30 m spatial resolutions and 5 day temporal resolutions. Using these products may decrease the error associated with satellite differences.

4.3 Interannual and Seasonal Water Quality Trends

Interannual variability in the *in situ* data was well represented in the out of sample model predictions. The correspondence between the seasonal trends in *in situ* data and modeled values were less clear, with patterns diverging in the winter. In the winter, *in situ* Secchi depths were high, whereas model Secchi depths ranged from low to high. The distribution of data over the course of the year differed between the two datasets, making trends difficult to compare. However, the divergence in trends may also indicate a weakness of *in situ* sampling that can be partially relieved by satellites.

In the field, measurements are not taken on stormy days because researchers cannot easily access field sites. Although satellites experience a similar sampling bias and are unable to capture useable data over water obscured by clouds, they can capture data if there are clear patches over sites of interest. It is possible that the satellites captured more turbid observations (from increased mixing in stormy weather) that *in situ* sampling missed.

4.4 Data Considerations

Observed *in situ* Secchi depths can be affected by reduced visibility from waves, cloud cover, poor eyesight by the observer, and sun position. Satellite measurements are also imperfect, being affected by adjacency effects from nearby land or back-scattering from the seafloor. Our model was also based off of observations that fell in an up to an 8 day temporal window, limiting the ability to make strong inferences about a particular day.

Investigating why satellite data could not be retrieved from certain coastal sites would contribute to the understanding of spatial limitations in satellite data retrievals, allowing researchers to randomly sample sites for *in situ* validation without wasting time at sites without corresponding satellite data. A similarity between sites could have caused them to be masked during SeaDAS's l2gen processing. Cloud coverage is unlikely because data could not be extracted from these sites on clear sky days, and "depth" is unlikely because sites where radiances could/could not be captured varied in depth. When turbidity is high, pixels may erroneously be masked as clouds (Loisel et al., 2013), but masked sites were no more turbid than sites with satellite retrievals. All standard Level-2 quality flags should be investigated, including ATM (atmospheric correction failure), LAND (land masking), and HILT (very high or saturated radiance). Additionally, it would be useful to investigate the differences in ACOLITE's atmospheric correction method that allowed for the extraction of data from sites SeaDAS consistently masked.

4.5 Satellite Overestimation

Ideally, vicarious calibration of remote sensing products with *in situ* radiometric observations could help determine what step(s) of the algorithm was responsible for the overestimation. However, this work is often time consuming and costly, so it could be useful to consider other ways to investigate this question.

Luis et al. shows that the Lee et al. Z_{SD} algorithm worked well for three coastal bodies in Boston but poorly in Boston Harbor. Perhaps shared characteristics affected the accuracy of satellite retrievals in the VCR and Boston Harbor. In their study, the effect of daily tides and proximity of stations to land was considered as a possible cause for satellite overestimation; however, neither limiting the temporal window to three hours or removing near shore stations significantly improved the satellite's estimates (Luis et al. 2019).

One possible solution is using an alternative algorithm for the calculation of inherent optical properties (IOPs) instead of the Quasi-Analytical Algorithm v6. Any errors in IOPs would propagate in the calculation of satellite Secchi depths. For example, Yang et al. created an alternative QAA (QAA turbid) because it has been found that the QAA can fail in some turbid waters (Lee et al., 2009; Yang et al., 2013).

$R_{rs}(665)$ is the reference wavelength used in the QAA. It is interesting that the anomalously high Secchi depth (site 6, 7/20/2019) yielded using SeaDAS and ACOLITE was associated with an anomalously low $R_{rs}(665)$. It would be interesting to compare R_{rs} retrievals from the VCR with R_{rs} retrievals from other turbid waters where the algorithm performed more accurately.

5. CONCLUSION

Our results demonstrate the ability of high-resolution satellite imagery to improve coastal water quality studies, as well as the need to further improve and calibrate ocean color algorithms for complex waters. Our model can be used to study spatiotemporal variability in water clarity in the Virginia Coast Reserve. Our modeling methods can be implemented in other water bodies to yield more accurate Secchi depths in the case of $Z_{SD,sat}$ overestimation.

ACKNOLEDGEMENTS

This work was funded by the Virginia Space Grant Consortium and the National Science Foundation's Research Experience for Undergraduates (REU) program. We are grateful to Kelly Luis at the University of Massachusetts Boston, who provided scripts for the implementation of the algorithms. Thank you to the researchers and staff of the University of Virginia's Anheuser-Busch Coastal Research Center, especially Karen McGlathery, John Porter, Robert Christian, Cora Baird, Carolyn Lewis, and Jonah Morreale.

REFERENCES

[1] Álvarez-Romero, J. G., Wilkinson, S. N., Pressey, R. L., Ban, N. C., Kool, J., & Brodie, J. (2014). Modeling catchment nutrients and sediment loads to inform regional management of water quality in coastal-marine ecosystems: A comparison of two approaches. Journal of Environmental Management, 146, 164–178. https://doi.org/10.1016/j.jenvman.2014.07.007

[2] Ben Hamner and Michael Frasco (2018). Metrics: Evaluation Metrics for Machine Learning. R package version 0.1.4. https://CRAN.R-project.org/package=Metrics

[3] Bierman, P., Lewis, M., Ostendorf, B., & Tanner, J. (2011). A review of methods for analysing spatial and temporal patterns in coastal water quality. *Spatial Information and Indicators for Sustainable Management of Natural Resources*, *11*(1), 103–114. https://doi.org/10.1016/j.ecolind.2009.11.001
[4] Carr, J., D'Odorico, P., McGlathery, K., & Wiberg, P. (2010). Stability and bistability of seagrass ecosystems in shallow coastal lagoons: Role of feedbacks with sediment resuspension and light attenuation. *Journal of Geophysical Research: Biogeosciences*, *115*(G3). https://doi.org/10.1029/2009JG001103
[5] Chen, J., Han, Q., Chen, Y., & Li, Y. (2019). A Secchi Depth Algorithm Considering the Residual Error in Satellite Remote Sensing Reflectance Data. *Remote Sensing*, *11*(16). https://doi.org/10.3390/rs11161948
John Fox and Sanford Weisberg (2019). An {R} Companion to Applied Regression, Third Edition. Thousand Oaks CA: Sage. URL: https://socialsciences.mcmaster.ca/jfox/Books/Companion/
[6] J. Masek, J. Ju, J. Roger, S. Skakun, M. Claverie, & J. Dungan. (2018). Harmonized Landsat/Sentinel-2 Products for Land Monitoring. *IGARSS 2018 - 2018 IEEE International Geoscience and Remote Sensing Symposium*, 8163–8165. https://doi.org/10.1109/IGARSS.2018.8517760
[7] Lee, Z., Carder, K.L., Arnone, R.A., 2002. Deriving inherent optical properties from water color: a multiband quasi-analytical algorithm for optically deep waters. Appl. Opt. 41 (27), 5755. https://doi.org/10.1364/AO.41.005755.
[8] Lee, Z.-P. (2005). A model for the diffuse attenuation coefficient of downwelling irradiance. Journal of Geophysical Research, 110(C2). http://dx.doi.org/10.1029/2004jc002275
[9] Lee, Z., Shang, S., Hu, C., Du, K., Weidemann, A., Hou, W., Lin, G., 2015. Secchi disk depth: a new theory and mechanistic model for underwater visibility. Remote Sens. Environ. 169, 139–149. https://doi.org/10.1016/j.rse.2015.08.002.
[10] Lee, Z., Shang, S., Qi, L., Yan, J., Lin, G., 2016. A semi-analytical scheme to estimate Secchi- disk depth from Landsat-8 measurements. Remote Sens. Environ. 177, 101–106. https://doi.org/10.1016/j.rse.2016.02.033.
[11] Liu, X., Lee, Z., Zhang, Y., Lin, J., Shi, K., Zhou, Y., Qin, B., & Sun, Z. (2019). Remote Sensing of Secchi Depth in Highly Turbid Lake Waters and Its Application with MERIS Data. *Remote Sensing*, *11*(19). https://doi.org/10.3390/rs11192226
[12] M A Luis, Kelly & Rheuban, Jennie & Kavanaugh, Maria & Glover, David & Wei, Jianwei & Lee, Zhongping & Doney, Scott. (2019). Capturing coastal water clarity variability with Landsat 8. Marine Pollution Bulletin. 145. 96-104. 10.1016/j.marpolbul.2019.04.078.
[13] Loisel, H., Vantrepotte, V., Jamet, C., & Dat, D. N. (2013). Challenges and New Advances in Ocean Color Remote Sensing of Coastal Waters. In Topics in Oceanography (pub.1050086998). https://doi.org/10.5772/56414
[14] McGlathery, K. and R. Christian. 2020. Water Quality Sampling - integrated measurements for the Virginia Coast, 1992-2019. Virginia Coast Reserve Long-Term Ecological Research Project Data Publication knb-lter-vcr.247.14 (doi:10.6073/pasta/db7f8fe720ddfcdfab1352adc9c22702).
[15] McGlathery KJ, Sundbäck K, Anderson IC (2007) Eutrophication in shallow coastal bays and lagoons: the role of plants in the coastal filter. Mar Ecol Prog Ser 348:1-18. https://doi.org/10.3354/meps07132
[16] Morel, André & Antoine, David & Gentili, Bernard. (2002). Bidirectional Reflectance of Oceanic Waters: Accounting for Raman Emission and Varying Particle Scattering Phase Function. Applied optics. 41. 6289-306. 10.1364/AO.41.006289.
[17] Pahlevan, N., Sarkar, S., Franz, B. A., Balasubramanian, S. V., & He, J. (2017). Sentinel-2 MultiSpectral Instrument (MSI) data processing for aquatic science applications: Demonstrations and validations. *Remote Sensing of Environment*, *201*, 47–56. https://doi.org/10.1016/j.rse.2017.08.033
[18] Preisendorfer, R. W. (1986). Secchi disk science: Visual optics of natural waters1. *Limnology and Oceanography*, *31*(5), 909–926. https://doi.org/10.4319/lo.1986.31.5.0909
[19] R Core Team (2013). R: A language and environment for statistical computing. R Foundation for Statistical Computing, Vienna, Austria. ISBN 3-900051-07-0, URL http://www.R-project.org/.
[20] Safak, I., Wiberg, P. L., Richardson, D. L., & Kurum, M. O. (2015). Controls on residence time and exchange in a system of shallow coastal bays. *Continental Shelf Research*, *97*, 7–20. https://doi.org/10.1016/j.csr.2015.01.009
[21] Simpson, G. L. (2018). Modelling Palaeoecological Time Series Using Generalised Additive Models. Frontiers in Ecology and Evolution, 6, 149. https://doi.org/10.3389/fevo.2018.00149
[22] Werdell, P.J., & McClain, C. R. (2019). Satellite Remote Sensing: Ocean Color☆. In J. K. Cochran, H. J. Bokuniewicz, & P. L. Yager (Eds.), Encyclopedia of Ocean Sciences (Third Edition) (pp. 443–455). Academic Press. https://doi.org/10.1016/B978-0-12-409548-9.10817-6